ORGANIC LETTERS

2013
Vol. 15, No. 14
3602–3605

Sesquiterpenoids with New Carbon Skeletons from the Resin of *Toxicodendron vernicifluum* as New Types of Extracellular Matrix Inhibitors

Jiang-Bo He,[†,‡] Jie Luo,[†] Li Zhang,[§] Yong-Min Yan,[†,‡] and Yong-Xian Cheng*[,†]

State Key Laboratory of Phytochemistry and Plant Resources in West China, Kunming Institute of Botany, Chinese Academy of Sciences, Kunming 650201, Yunnan, P. R. China, University of Chinese Academy of Sciences, Beijing 100049, P. R. China, and Institute of Materia Medica, Chinese Academy of Medical Sciences, Beijing 100050, P. R. China

yxcheng@mail.kib.ac.cn

Received May 23, 2013; Revised Manuscript Received June 24, 2013

ABSTRACT

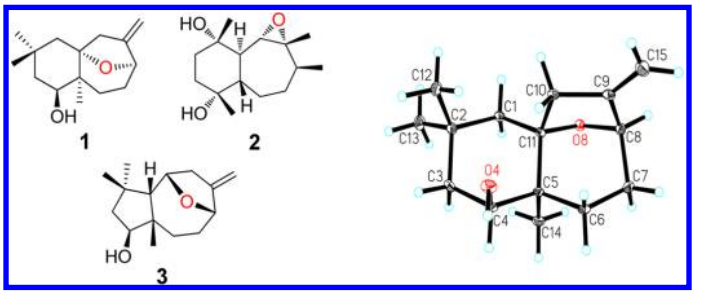

Toxicodenanes A−C (1−3), representing sesquiterpenoids with three new carbon skeletons, were isolated from the dried resin of *Toxicodendron vernicifluum*. Their structures were identified by spectroscopic data and X-ray diffraction crystallography. Their plausible biosynthetic route was proposed via the isolated intermediate (4). Compounds 2 and 3 could significantly inhibit overproduction of fibronectin, collagen IV, and IL-6 in high-glucose-induced mesangial cells in a dose- and time-dependent manner, showing their potential in diabetic nephropathy.

Diabetic nephropathy (DN) is a major and serious complication of diabetes mellitus (DM), which affects 20% to 30% of patients with DM in their lifetime.[1] Due to the large prevalence of DM in the general population, the patients suffering from DN are increasing rapidly. DN as a consequence of DM in turn has become the most common cause of end-stage renal disease (ESRD), accounting for more than half of all cases of ESRD in the United States.[2]

For patients with ESRD, hemodialysis is an expedient measure but a heavy economic burden to patients. Renal transplantation is an ultimate way out but meets with the big challenge of kidney supply and demand. As a consequence, the majority of patients with ESRD die during a waiting process. Evidence suggests that retarding the progression of DN will alleviate the conflicts between kidney supply and demand. Unfortunately, clinically available drugs for DN are scarce, and the data from Thomson Reuters Pharma showed that compounds launched in different research and development phases are no more than 100, of which only 2 are in phase III clinical trials. Therefore, an urgent need exists to identify new natural products with effects on DN which will provide new structure templates for drug optimization.

Resins are secreted by many plants, and their biological effects and defensive roles in the plants have been widely documented.[3] Gambogic acid, for example, as a xanthonoid derived from the resin of *Garcinia hanburyi*, is well-known for its profound antitumor activity in clinical trials

[†] Kunming Institute of Botany, Chinese Academy of Sciences.
[‡] University of Chinese Academy of Sciences.
[§] Institute of Materia Medica, Chinese Academy of Medical Sciences.

(1) Thorp, M. L. *Am. Fam. Physician* **2005**, *72*, 96–99.
(2) Molitch, M. E.; DeFronzo, R. A.; Franz, M. J.; Keane, W. F.; Mogensen, C. E.; Parving, H. H.; Steffes, M. W. *Diabetes Care* **2000**, *23*, S69–S72.

10.1021/ol4014415
Published on Web 07/01/2013

and rodent experimental models.[4] *Resina Toxicodendri* (ResT) is the dried resin produced by *T. vernicifluum* which is known as Chinese lacquer tree growing in East Asia and largely cultivated for its toxic sap. As ResT is used as a Chinese medicine for promoting blood circulation and removing blood stasis, it always occurs in prescriptions of Chinese medicine. We hypothesized that ResT might contain compounds which are beneficial for DN because DN is a microvascular-associated disease. With this motivation, we investigated the ethanol extract of ResT, from which three new sesquiterpenoids, toxicodenanes A–C (**1**–**3**), representing three new carbon skeletons, were isolated and structurally identified. Toxicodenanes A and B (**1** and **2**) possess a 6/7 ring system, and toxicodenane C (**3**) bears a 5/8 ring system. Both **1** and **3** have a tetrahedron furan ring moiety in the molecules which made them cage-like structures. Since oversecretion of extracellular matrix and proinflammatory factors are definitely implicated in DN, these isolates were purposely screened for their anti-diabetic nephropathy potential by using high-glucose-induced mesangial cells. Here, the isolation and structural elucidation of compounds **1**–**3**, representing the first example of three new classes of sesquiterpenoids, are reported as well as their antidiabetic nephropathy activity.

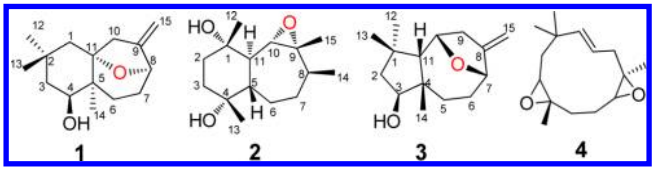

Compound **1**[5] was isolated as colorless crystals (CH_3OH). Its molecular formula was established as $C_{15}H_{24}O_2$ by HRESIMS (*m*/*z* 235.1696 $[M - H]^-$, calcd for 235.1698), requiring four degrees of unsaturation. The IR spectrum displayed the existence of hydroxyl (3409 cm^{-1}) and double bond (1669 cm^{-1}) groups. The ^1H NMR spectroscopic data of **1** (Table 1 in the Supporting Information (SI)) revealed the presence of three single methyl [δ_H 0.96 (3H, s, H-12), 1.16 (3H, s, H-13), 1.08 (3H, s, H-14)] and two terminal olefinic protons [δ_H 4.84 and δ_H 4.79 (each 1H, s, H-15a and H-15b)]. The ^{13}C NMR and DEPT spectroscopic data (Table 1 in the SI) of **1** indicated 15 carbon resonances, including three methyl, six methylene (including one terminal double bond), two oxygenated methine, and four quaternary carbons (including one oxygenated sp^3 quaternary carbon, one sp^2 quaternary carbon). Inspection of the ^1H and ^{13}C NMR spectra of **1** indicated a sesquiterpenoid. The total NMR spectroscopic data of **1** were assigned by a combined analyses of 1D and 2D NMR spectra including HSQC, HMBC, and $^1H-^1H$ COSY spectra. The $^1H-^1H$ COSY correlations (Figure 1) of H-3/H-4 and H-6/H-7/H-8 displayed the key spin systems. In the HMBC spectrum (Figure 1), the correlations from H-12 and H-13 to C-1, C-2, and C-3 indicated that the 12-CH_3 and 13-CH_3 were both connected to C-2; the correlations from H-14 to C-4, C-5, C-6, and C-11 suggested that the 14-CH_3 was linked to C-5; the correlations from H-15a and H-15b to C-8, C-9, and C-10 confirmed the presence of the terminal double bond in the molecule, which was established to be located at C-9. The two oxymethine carbons and one oxygenated quaternary carbon were assigned to C-4, C-8, and C-11 from its downfield chemical shifts, along with the HMBC and $^1H-^1H$ COSY correlations. Apart from one double bond and two carbon ring systems, the remaining unsaturation in **1** was assumed to be representative of an oxygen bridge between C-11 and C-4 or C-11 and C-8, forming another ring system. The oxygen bridge was deduced to be between C-11 and C-8 from the HMBC correlation from H-8 to C-11, forming a cage-like structure.

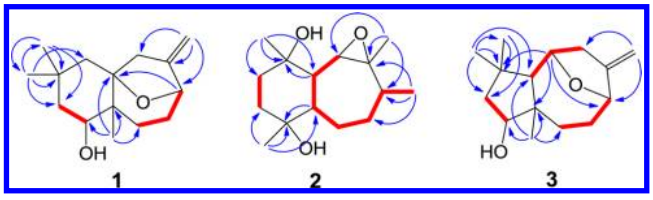

Figure 1. Key HMBC (blue arrows) and $^1H-^1H$ COSY (red lines) correlations of **1**–**3**.

The relative configuration of **1** was assigned by ROESY experiments and X-ray crystallographic diffraction. In the ROESY spectrum (Figure 2), the correlations of H-14/H-4 and H-14/H-12 indicated that 14-CH_3, 12-CH_3, and H-4 were on the same side of the ring, possessing α-orientation. The strong correlation of H-8 with H-10a (δ_H 3.62) indicated that the oxygen bridge was on the same side. H-8 was determined to be *β*-oriented based on the correlations of H-10a/H-13 and H-10a/H-8 as shown in the molecular model. The structure and relative configuration of **1** were finally confirmed by a single-crystal X-ray diffraction (Figure 3)[6] using anomalous scattering of Cu Kα radiation, which indicated that compound **1** is a racemic mixture, comprised of equal amounts of left- and right-handed enantiomers (4*S*, 5*S*, 8*R*, 11*R* and 4*R*, 5*R*, 8*S*, 11*S*). Therefore, the structure of **1** was established and named (±)-toxicodenane A.

Compound **2**,[7] obtained as a colorless gum, was determined to have the molecular formula $C_{15}H_{26}O_3$ by HRESIMS (*m*/*z* 253.1802 $[M - H]^-$, calcd for 253.1803), with three degrees of unsaturation. The IR spectrum of **2**

(3) (a) Schmidt, T. J.; Kaiser, M.; Brun, R. *Planta Med.* **2011**, *77*, 849–850. (b) Salatino, A.; Fernandes-Silva, C. C.; Righi, A. A.; Salatino, M. L. F. *Nat. Prod. Res.* **2011**, *28*, 925–936. (c) Langenheim, J. H., *Plant Resins: Chemistry, Evolution, Ecology, and Ethnobotany*; Timber Press: Portland, OR, 2003.

(4) Zhang, X. J.; Li, X.; Sun, H. P.; Wang, X. J.; Zhao, L.; Gao, Y.; Liu, X. R.; Zhang, S. G.; Wang, Y. Y.; Yang, Y. R.; Zeng, S.; Guo, Q. L.; You, Q. D. *J. Med. Chem.* **2013**, *56*, 276–292.

(5) (±)-Toxicodenane A (**1**): colorless crystals; $[\alpha]^{15}_D$ − 11.9 (this may result from the residual impurity) (*c* 0.1, $CHCl_3$); IR (KBr) ν_{max} 3409, 2955, 2924, 2857, 1669, 1463, 1377, 1173, 1124, 1050, 1033, 1008, 763 cm^{-1}; ^1H and ^{13}C NMR spectroscopic data, see SI; ESIMS: (negative) *m*/*z* 235 $[M - H]^-$; HRESIMS: *m*/*z* 235.1696 $[M - H]^-$ (calcd for $C_{15}H_{23}O_2$, 235.1698).

(6) Crystallographic data of (±)-toxicodenane A (**1**) have been deposited at the Cambridge Crystallographic Data Centre (Deposition No. CCDC 926067). Copies of these data can be obtained free of charge via www.ccdc.cam.an.uk/conts/retrieving.html.

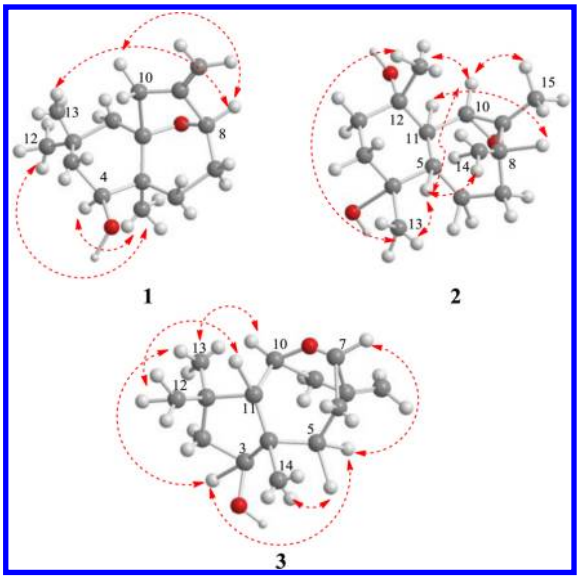

Figure 2. ROESY (red arrows) correlations of **1**–**3**.

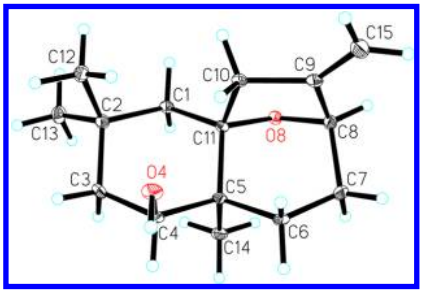

Figure 3. X-ray crystallographic structure of **1**.

revealed the presence of a hydroxyl group (3423 cm^{-1}). The ^1H NMR showed four methyl [δ_H 1.33 (3H, s, H-12), 1.13 (3H, s, H-13), 1.00 (3H, d, J = 7.2 Hz, H-14), 1.21 (3H, s, H-15)] signals. The ^{13}C and DEPT NMR data of **2** (see SI) also showed 15 carbon resonances, indicating a sesquiterpenoid skeleton. The $^1H-^1H$ COSY (Figure 1) correlations of H-2/H-3 and H-10/H-11/H-5/H-6/H-7/H-8/H-14 revealed two spin systems. In the HMBC spectrum (Figure 1), the correlations from H-12 to C-1, C-2, and C-11 and from H-13 to C-3, C-4, and C-5 indicated that 12-CH_3 and 13-CH_3 were connected to C-1 and C-4, respectively. The HMBC correlations from H-14 to C-7, C-8, and C-9 and correlations from H-15 to C-8, C-9, and C-10 suggested that 14-CH_3 and 15-CH_3 were located at C-8 and C-9, respectively. C-9 and C-10 were oxygen-bearing carbons based on their downfield chemical shifts in the ^{13}C NMR spectrum. Analysis of the unsaturation of **2** revealed the presence of another epoxy group in this molecule, as there were only two carbon rings deduced by the HMBC and $^1H-^1H$ COSY correlations. Thus, the planar structure of **2** was determined as shown, with a 6/7 ring sesquiterpenoid.

The relative configuration of **2** was established by ROESY experiments. In the ROESY spectrum (Figure 2), the correlations of H-5/H-10, H-13, H-12/H-10, H-13 indicated the β-orientation of H-5, H-10, 12-CH_3, and 13-CH_3. 14-CH_3 and 15-CH_3 were deduced to be β-oriented from the correlations of H-15/H-10, H-14, which were further confirmed by the correlation of H-14/H-12, H-13. The α-orientation of H-11 was assigned by the correlation of H-11/H-8. Therefore, the structure of **2** was assigned as shown, named toxicodenane B.

Compound **3**[8] possessed the same molecular formula as that of **1**, deduced from the HREIMS (m/z 236.1778 $[M]^+$, calcd for $C_{15}H_{24}O_2$, 236.1776), indicating 4 degrees of unsaturation. The IR spectrum showed the presence of hydroxyl (3426 cm^{-1}) and double bond (1640 cm^{-1}) groups. The ^1H NMR spectrum of **3** was similar to that of **1**, suggesting a sesquiterpenoid, with three single methyl [δ_H 1.09 (3H, s, H-12), 1.14 (3H, s, H-13), 1.02 (3H, s, H-14)] and two terminal olefinic protons [δ_H 4.95 (1H, d, J = 2.0 Hz, H-15a) and δ_H 4.90 (1H, d, J = 2.0 Hz, H-15b)]. The ^{13}C NMR and DEPT spectroscopic data of **3** (see SI) were also highly similar to those of **1**, except that the oxygenated quaternary carbon at C-11 in **1** was replaced by an oxymethine at C-10 (δ_C 78.2) in **3**, which was established by the HMBC correlations (Figure 1) from H-10 to C-1 and C-4, along with the $^1H-^1H$ COSY correlations (Figure 1) of H-9/H-10/H-11. Furthermore, another major difference between these two compounds was that the methylene signal at C-1 in **1** was replaced by a methine at C-11 (δ_C 64.1) in **3**, which was determined on the basis of the HMBC correlations from H-12 and H-13 to C-1, C-2, and C-11 and from H-14 to C-3, C-4, C-5, and C-11. The HMBC correlations from H-15a and H-15b to C-7, C-8, and C-9 confirmed that the terminal double bond was located at C-8. The hydroxyl group was deduced to be located at C-3 based on the downfield chemical shift and the HMBC correlation from H-14 to C-3, together with the $^1H-^1H$ COSY correlation of H-2/H-3. The key HMBC correlation from H-10 to C-7 confirmed that the oxygen bridge was between C-10 and C-7, in accordance with the molecular formula revealed by the HREIMS and the degrees of unsaturation in the molecule. The formation of the oxygen bridge made the structure cage-like.

The relative configuration of **3** was assigned by ROESY experiment. In the ROESY spectrum (Figure 2), the correlations of H-13/H-3, H-10, and H-12/H-11 indicated the α-orientation of H-10, 13-CH_3, and H-3 and the β-orientation of 12-CH_3 and H-11. The β-orientation of 14-CH_3 was assigned by the correlations of H-3/H-5a (δ_H 2.09) and H-14/H-5b (δ_H 1.56). Therefore, the structure of **3** was assigned as shown, named toxicodenane C.

(7) Toxicodenane B (**2**): colorless gums; $[\alpha]^{15}_D$ +7.69 (c 0.24, $CHCl_3$); IR (KBr) ν_{max} 3423, 2958, 2924, 2853, 1727, 1462, 1377, 1159, 1065, 1033, 968 cm^{-1}; ^1H and ^{13}C NMR spectroscopic data, see SI; ESIMS (negative): m/z 507 $[2M - H]^-$; HRESIMS (negative): m/z 253.1802 $[M - H]^-$ (calcd for $C_{15}H_{25}O_3$, 253.1803).

(8) Toxicodenane C (**3**): colorless gums; $[\alpha]^{15}_D$ – 4.9 (c 0.35, CHCl3); IR (KBr) ν_{max} 3426, 2954, 2925, 2854, 1640, 1463, 1378, 1168, 1093, 1042, 1033, 881 cm^{-1}; ^1H and ^{13}C NMR spectroscopic data, see SI; EIMS: m/z 236 $[M]^+$; HREIMS: m/z 236.1778 $[M]^+$ (calcd for $C_{15}H_{24}O_2$, 236.1776).

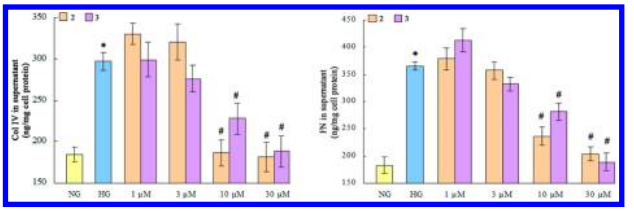

Figure 4. Compounds inhibited collagen IV and fibronectin production in a dose-dependent manner; $^{*}p < 0.05$ vs NG; $^{\#}p < 0.05$ vs HG.

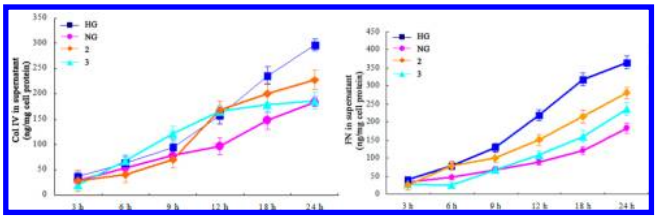

Figure 5. Compounds inhibited collagen IV and fibronectin production in a time-dependent manner at 10 μM.

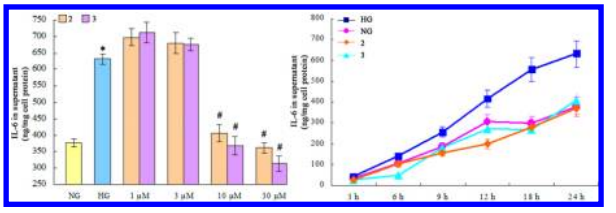

Figure 6. Compounds inhibited IL-6 production in a dose- (left) and time- (right) dependent manner; $^{*}p < 0.05$ vs NG; $^{\#}p < 0.05$ vs HG.

Excessive accumulation of the extracellular matrix (fibronectin, collagen IV, etc.) in the glomerular mesangium is the major pathologic feature of DN and a cause of renal fibrosis or glomerulosclerosis. Therefore it has been considered as a crucial therapeutic target of DN.[9] Chronic inflammation is definitely implicated in DN.[10] Therefore, inhibition of proinflammatory factors (such as cytokin IL-6) will be beneficial for arresting the progression of DN. In this study, compounds **2** and **3** were examined for their inhibitory effects in high-glucose-induced mesangial cells.

As shown in Figures 4 and 5, high glucose levels induced overproduction of fibronectin (FN) and collagen IV (col IV) but this overproduction was significantly inhibited by pretreating mesangial cells with **2** and **3**. In addition, the inhibitory effects of **2** and **3** were both dose- and time-dependent. As shown in Figure 6, the high-glucose-induced overproduction of IL-6 was also alleviated significantly by

(9) Mason, R. M.; Wahab, N. A. *J. Am. Soc. Nephrol.* **2003**, *14*, 1358–1373.
(10) Tuttle, K. R. *J. Am. Soc. Nephrol.* **2005**, *16*, 1537–1538.

Scheme 1. Plausible Biogenetic Route of **1** and **3**

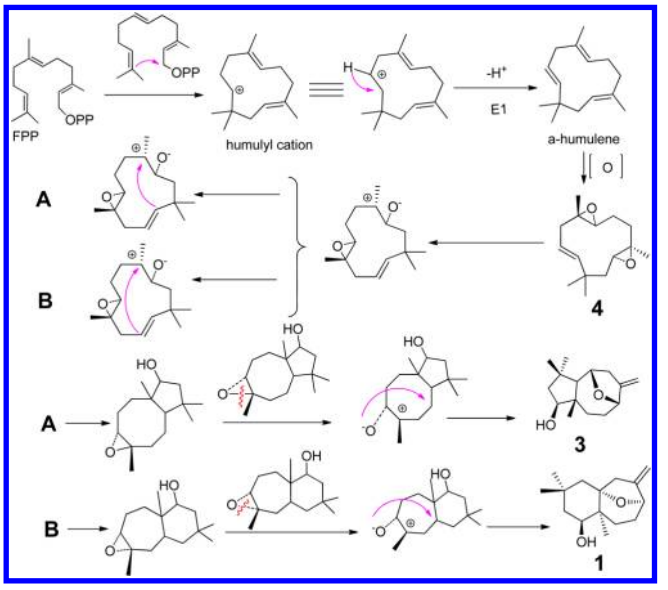

pretreating mesangial cells with **2** and **3**. TGF-beta/Smads pathway is a critical pathway, but we found that the inhibitory effects of **2** and **3** are not via this pathway. As many signal pathways are involved in DN, the mode of action requires further investigation. In addition, to exclude the effects of **2** and **3** as being caused by their cellular toxicity, a cytotoxicity assay was performed in every experiment. The results showed that there was no significant difference among the groups (data not shown).

The isolate **4** was derived from α-humulene, which is formed from a common farnesyl prophosphate by an enzymatic cyclization reaction. We suggested that compounds **1** and **3** started from **4**. Oxidation of **4** followed by carbon bond formation led to A (5/8 ring system) and B (6/7 ring system). Starting from A and B, the formation of the oxygen bridge led to **3** and **1**, respectively.

A plausible biogenetic pathway of **1** and **3** was proposed as shown in Scheme 1.

To our knowledge, natural products which regulated the extracellular matrix of mesangial cells are relatively rare. Compounds **2** and **3** might provide new structure templates for antidiabetic nephropathy drug optimization.

Acknowledgment. This project was supported financially by the NSFC-Joint Foundation of Yunnan Province (No. U1202222), and project support to Y.-X.C. from State Key Laboratory of Phytochemistry and Plant Resources in West China, Kunming Institute of Botany, Chinese Academy of Sciences (P2010-ZZ09 and P2013-ZZ03) is also acknowledged.

Supporting Information Available. Detailed experimental procedures, bioassay methods, 1D and 2D NMR, MS, and IR spectra of compounds **1**–**3**, X-ray crystal data of **1**, NMR data of **1**–**3**, and partial biological data. This material is available free of charge via Internet at http://pubs.acs.org.

The authors declare no competing financial interest.